Feasibility of band gap engineering of pyrite FeS_{2}

Ruoshi Sun and Gerbrand Ceder

Phys. Rev. B **84**, 245211 — Published 27 December 2011

DOI: 10.1103/PhysRevB.84.245211

Feasibility of band gap engineering of pyrite FeS_2

Ruoshi Sun and Gerbrand Ceder*
Department of Materials Science and Engineering,
Massachusetts Institute of Technology, Cambridge, Massachusetts, USA
(Dated: December 5, 2011)

We use first-principles computations to investigate whether the band gap of pyrite FeS_2 can be increased by alloying in order to make it a more effective photovoltaic material. In addition to the isostructural compounds that have a larger band gap (ZnS_2, RuS_2, OsS_2), we evaluate non-rare-earth isovalent alloying candidates among all metals, transition metals, and semiconductor elements up to group IV and period 6 in the periodic table. From this screening procedure, we find that the group II elements (Be, Mg, Ca, Sr, Ba) and Cd have higher band gaps in the pyrite structure than FeS_2. Practical band gap enhancement is observed only in the Ru and Os alloyed systems, but their incorporation into pyrite may be severely limited by the large positive enthalpy of mixing. All other candidate $(Fe, M)S_2$ systems exhibit very large gap bowing effects such that the band gap at intermediate compositions is even lower than that of FeS_2. Positive correlations between immiscibility and differences in electronegativity and Shannon ionic radius are observed.

PACS numbers: 71.15.Mb, 71.20.Nr, 72.40.+w

I. INTRODUCTION

Being almost 0.5 eV less than the optimum band gap (1.4 eV) within Shockley-Queisser theory,[1] the band gap of pyrite FeS_2 ($E_g^{\rm expt} = 0.95$ eV; see Ref. 2) is suboptimal for single-junction photovoltaic applications, and it is of interest to understand to what extent this gap can be modified. Following our recent studies on the bulk, surface, interfacial,[3] and point defect properties[4] of pyrite, we investigate in this manuscript whether the long-standing problem of its low open-circuit voltage (OCV) can be mediated by band gap engineering.

It is common practice to tune the electronic properties of semiconductors by alloying.[5,6] The idea of alloying pyrite with a higher-gap material to enhance the low OCV is first mentioned in the work of Altermatt *et al.*, in which the incorporation of Zn is suggested as a target for future work.[7] Although the band gap of ZnS_2 has not been experimentally determined, it is estimated to be 2.5 eV.[8] Other known isostructural disulfides include MnS_2, CoS_2, NiS_2, CuS_2, RuS_2, and OsS_2. (See Ref. 2 and references therein.) Among these materials, MnS_2,[2] CoS_2, and CuS_2 are metallic,[9] and NiS_2 has a smaller band gap than pyrite,[2] making them of little interest to increase the band gap of pyrite. This leaves ZnS_2, RuS_2 ($E_g^{\rm expt} = 1.3$ eV; Ref. 2), and OsS_2 ($E_g^{\rm expt} = 2.0$ eV; Ref. 2) as remaining candidates.

Solid solutions of various isostructural pyrite materials, e.g., $(Fe, Co)S_2$, $(Fe, Ni)S_2$, and $(Fe, Cu)S_2$, have been synthesized,[10,11] though their band gaps have not been evaluated. Elements that do not form the pyrite crystal structure with S can, in principle, also be used as alloying additions to FeS_2, although in many cases their enthalpy of mixing is large.

In the remaining sections, we first describe the computational techniques in Sec. II A, the analysis framework in Sec. II B, and the materials screening procedure in Sec. II C. Results for alloying pyrite with elements that form (do not form) the pyrite crystal structure are shown in Sec. III A (Sec. III B). In Sec. IV, we discuss our findings and show correlations between electronegativity difference, size difference, band gap bowing, and miscibility.

II. METHODS

A. Computational details

Density-functional theory (DFT)[12,13] calculations within the Perdew-Burke-Ernzerhof (PBE)[14,15] generalized gradient approximation (GGA) were performed using the plane-wave code Vienna Ab-initio Simulation Package (VASP)[16–19] with projector augmented wave (PAW) potentials.[20,21] Total energies were converged to within 10^{-6} and 10^{-4} eV for each self-consistent loop and ionic relaxation step, respectively, using an $8 \times 8 \times 8$ Monkhorst-Pack[22] grid of k-points. For each mixture, the calculated equilibrium lattice constant (a_0), the bulk modulus (B), and the pressure derivative of the bulk modulus (B') were obtained by fitting the total energy of the relaxed structure at different volumes to the Murnaghan equation of state (EOS):[23]

$$E(V) = E(V_0) + \frac{BV}{B'}\left[\frac{(V_0/V)^{B'}}{B'-1} + 1\right] - \frac{BV_0}{B'-1}, \tag{1}$$

where V_0 is the equilibrium volume.

The band gap was obtained using the Δ-sol method[24] with an $8 \times 8 \times 8$ Γ-centered mesh of k-points:

$$E_g = \frac{E(N_0 + n) + E(N_0 - n) - 2E(N_0)}{n}, \tag{2}$$

where N_0 is the number of valence electrons in the original $(Fe, M)S_2$ unit cell, $n = N_0/N^*$, $N^* = 72$, and total energies $E(N_0)$ and $E(N_0 \pm n)$ were calculated at the experimental lattice constants whenever known, as recommended in Ref. 24. For mixtures of compounds whose experimental lattice constant is known for both end members in the pyrite structure, the gap of the mixture was calculated at the lattice constant linearly interpolated between the end members. For other mixtures where this information is not available, the calculated lattice constant was used. It is important to note that we do not use DFT band gaps calculated with local and semilocal functionals for screening, since they underestimate the band gap. On the other hand, it has been demonstrated in Ref. 24 that the band gap error in the Δ-sol method is only $O(0.1)$ eV, on par with results from the hybrid functional HSE06,[25,26] but the computational cost of Δ-sol is similar to a typical DFT calculation, making it the method of choice for high-throughput band gap screening.

We used 12-atom unit cells in all calculations. Band structures were computed following Ref. 3.

B. Analysis framework

We fit the lattice constant, bulk modulus, and band gap of the $Fe_xM_{1-x}S_2$ pseudobinary mixtures with a quadratic function of the concentration x:

$$P(x) = xP(0) + (1-x)P(1) - b_P\ x(1-x), \tag{3}$$

where P is the relevant property and b_P is its bowing parameter. The bowing parameters b_a, b_B, and b_g were obtained by fitting the lattice constant, bulk modulus, and band gap of $Fe_xM_{1-x}S_2$, for $x = 0, 0.25, 0.5, 0.75, 1$, respectively. In particular, if $b_a \approx 0$ then the alloy obeys Vegard's rule.

To obtain information on the miscibility of FeS_2 with the MS_2 alloying compound, the critical temperature at the top of the miscibility gap (T_c) was estimated as

$$T_c = \frac{\Omega}{2k_B}, \tag{4}$$

where Ω is the regular solution interaction parameter fitted to the calculated energies of mixing. Since the mixing enthalpy in the regular solution model is quadratic in concentration, Ω can also be viewed as the (negative of the) bowing parameter of $\Delta H(x)$.

Solutions can often be created in epitaxial conditions. To investigate this possibility we used the model of Ipatova *et al.*, who showed that, for a pseudobinary semiconductor film coherently grown on a lattice-matched substrate, the critical temperature for the spinodal instability at $x = 0.5$ is[27]

$$T_c^* = \frac{1}{2R}\left\{\Omega - \frac{(c_{11}-c_{12})(c_{11}+2c_{12})}{2(c_{11}+c_{12})} V_m \left[\frac{a(1)-a(0)}{a(0.5)}\right]^2\right\}, \tag{5}$$

where R is the gas constant, V_m is the molar volume, c_{ij}'s are elastic constants at $x = 0.5$ in Voigt notation, and the $a(x)$'s are the lattice constants at the corresponding concentrations. The elastic constants c_{11} and c_{12} in Eq. (5) were calculated by applying lattice distortions following Mehl.[28] It can be easily shown that, in cubic systems, the total strain energy associated with the applied strain

$$\epsilon_{ij} = \begin{pmatrix} \delta & 0 & 0 \\ 0 & -\delta & 0 \\ 0 & 0 & \delta^2/(1-\delta^2) \end{pmatrix} \tag{6}$$

takes the form

$$\Delta E = (c_{11} - c_{12}) V \delta^2 + O(\delta^4), \tag{7}$$

where ΔE is the total energy referenced to the unstrained system. Total energies were calculated at $\delta a_0 = 0, 0.2, 0.4, 0.6$ Å. Using the bulk modulus determined from the Murnaghan EOS [Eq. (1)] and the fact that $B = (c_{11} + 2c_{12})/3$ within linear elasticity, the elastic constants c_{11} and c_{12} were obtained and substituted into Eq. (5) to calculate T_c^*.

C. Screening procedure

For all known candidate compounds that are isostructural to FeS_2, only those that have a higher experimental gap (Zn, Ru, Os) were studied. Among elements that do not form the pyrite structure with S, we considered all isovalent metals, transition metals, and semiconductor elements up to group IV and period 6 in the periodic table as possible alloying additions. Non-isovalent materials were not considered since disulfides of cations that are not 2+ would not be charge compensated, thus moving the Fermi level into the conduction or valence band of FeS_2. Rare-earths were excluded from the screening procedure as their usage would reduce the potential economic competitiveness of pyrite[29] in large-scale photovoltaic applications. For each possible alloying element M, the band gap of the disulfide MS_2 in the (hypothetical) pyrite crystal structure was calculated using the Δ-sol method as described in Sec. II A. Materials that have a smaller gap were eliminated. The band gaps and formation energies at $x = 0.25, 0.5, 0.75$ were calculated for the remaining candidates.

A successful alloying material must meet the following criteria: (i) the band gap bowing parameter should be small (or negative) to increase the gap with as little alloying element as possible; (ii) the regular solution interaction parameter should be small to ensure miscibility; and (iii) the material should not be expensive.

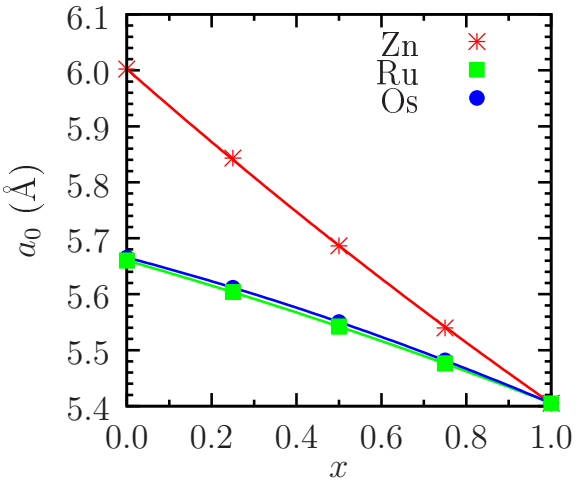

FIG. 1. (Color online) PBE lattice constant of $Fe_xM_{1-x}S_2$ as a function of x. The bowing parameters for M=Zn, Ru, and Os are $b_a = 0.0677$, -0.0382, and -0.0601 Å, respectively.

III. RESULTS

A. Elements that form pyrite structure with S: Zn, Ru, Os

The Murnaghan EOS is calculated at each composition (not shown) to give the computed lattice constant and bulk modulus. Figure 1 shows the lattice constant as a function of composition x. While the lattice parameter mostly obeys Vegard's law, the bulk modulus does not interpolate linearly with composition (Fig. 2). The bowing parameter b_B is on the order of 10 GPa.

As stressed in Ref. 24, it is important to calculate the band gap at the experimental lattice parameter rather than the computationally optimized lattice constant. Since the experimental lattice constants at intermediate compositions for these $(Fe, M)S_2$ systems are unknown, they must be interpolated from the end members. Based on the finding that the bowing parameter b_a is negligible [$O(0.01)$ Å; Fig. 1], we simply perform a linear interpolation between the experimental lattice constant for intermediate values of x (Table I). The calculated band gaps of $(Fe, M)S_2$ are shown in Fig. 3 for M=Zn, Ru, Os. For Zn alloying there is a considerable amount of band bowing ($b_g = 3.3$ eV), making it ineffective to increase the gap of FeS_2. Ru and Os seem to be favorable alloying additions, as the band gap increases monotonically with the solute concentration.

In Fig. 4 we show the miscibility of these systems by plotting the enthalpy of mixing (ΔH) as a function of concentration. The fitted regular solution interaction parameter is 851, 222, and 231 meV/FU for Zn, Ru, and Os, respectively. Using Eq. (4), the critical temperature at the top of the miscibility gap is estimated to be 4940, 1290, and 1340 K, respectively (Table II), which is well above the melting temperature of pyrite ($T_m = 1016$ K; see Ref. 2). The elastic constants calculated at $x = 0.5$ and the critical temperature of the spinodal instability are also given in Table II.

Our results indicate that all three elements, Zn, Ru, and Os, may be difficult to incorporate in FeS_2. A similar problem has been identified when trying to design $(Fe, Mn)S_2$ mixtures in order to control the low-to-high spin transition.[30]

B. Elements that do not form pyrite structures with S

In principle, alloying elements obviously do not have to form the pyrite structure in their binary with S in order to be effective at increasing the gap of FeS_2. However, such potential alloying elements are less likely to be miscible. This can be observed by considering the total enthalpy of the mixing reaction,

$$\Delta H = \Omega x_{\mathrm{Fe}} x_{\mathrm{M}} + x_{\mathrm{M}} \Delta H_{p' \to \mathrm{pyrite}}, \tag{8}$$

which besides the regular-solution-like term now also contains a positive promotion energy to bring the M sulfide from its ground state phase p' to the pyrite structure. While we do not calculate $\Delta H_{p' \to \mathrm{pyrite}}$ for these elements, we find that the regular solution enthalpy alone is already quite limiting for mixing these elements into pyrite.

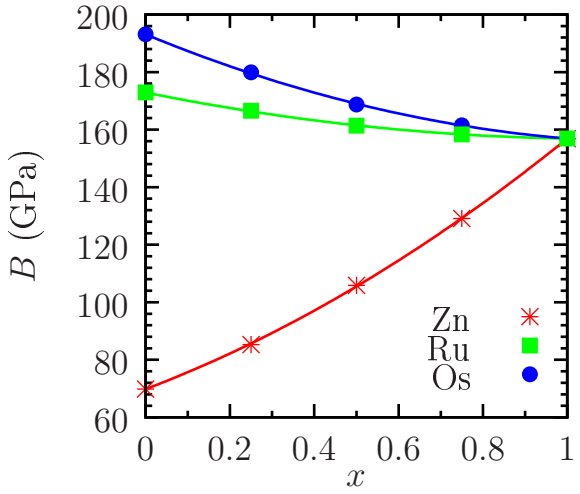

FIG. 2. (Color online) Bulk modulus of $Fe_xM_{1-x}S_2$ as a function of x. The bowing parameters for M=Zn, Ru, and Os are $b_B = 31.4$, 13.6, and 24.0 GPa, respectively.

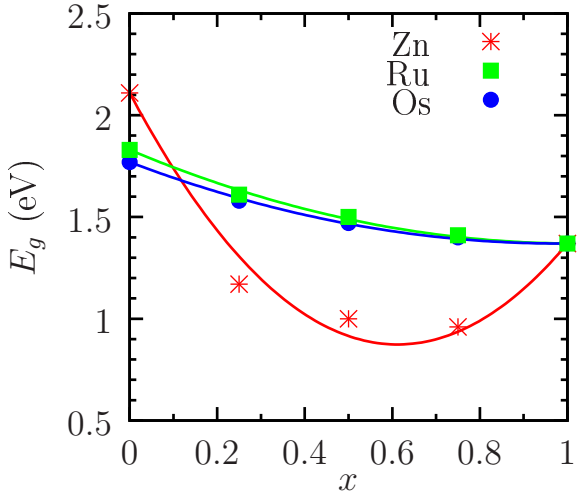

FIG. 3. (Color online) Band gap of $Fe_xM_{1-x}S_2$ as a function of x. The bowing parameters for M=Zn, Ru, and Os are $b_g = 3.3$, 0.44, and 0.41 eV, respectively.

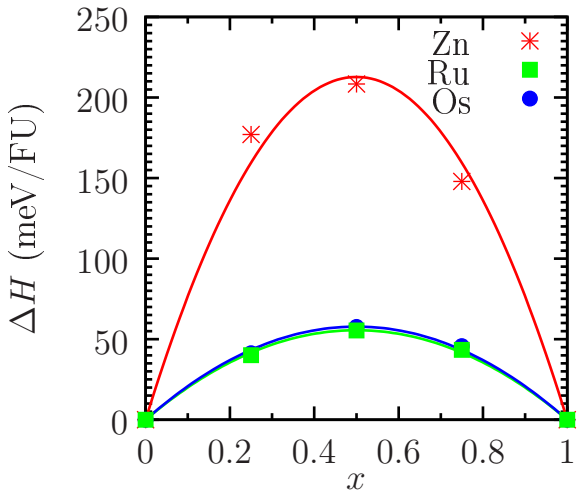

FIG. 4. (Color online) Mixing enthalpy of $Fe_xM_{1-x}S_2$ as a function of x. The bowing parameters for M=Zn, Ru, and Os are $\Omega = 851$, 222, and 231 meV/FU, respectively.

TABLE I. Lattice constants (a_0 as calculated within PBE; in Å), bulk modulus (B in GPa), pressure derivative of the bulk modulus (B'), and Δ-sol fundamental gap (E_g in eV) of $Fe_xM_{1-x}S_2$. Experimental values are given in brackets whenever available. The $x = 1$ data set refers to FeS_2. B and B' are given at the calculated lattice parameter while E_g is calculated at the lattice parameter that is linearly interpolated between the experimental lattice parameter of the end members.

M	x	a_0	B	B'	E_g
-	1	5.405 (5.416[a])	156.9	5.47	1.4 (0.95[b])
Zn	0.75	5.540	129.1	4.83	1.0
	0.5	5.686	105.9	4.66	1.0
	0.25	5.843	85.3	2.32	1.2
	0	6.002 (5.954[c])	69.8	5.04	2.1 (2.5[d])
Ru	0.75	5.476	158.3	4.93	1.4
	0.5	5.542	161.4	5.21	1.5
	0.25	5.603	166.6	4.79	1.6
	0	5.660 (5.611[e])	172.9	4.94	1.8 (1.3[b])
Os	0.75	5.482	161.5	4.92	1.4
	0.5	5.550	168.7	5.17	1.5
	0.25	5.612	179.9	4.61	1.6
	0	5.666 (5.619[f])	193.1	4.96	1.8 (2.0[b])

[a] Reference 31.
[b] Reference 2.
[c] Reference 11.
[d] Reference 8 (estimate).
[e] Reference 32.
[f] Reference 33.

TABLE II. Elastic constants (in GPa) and critical temperatures [T_c and T_c^* obtained from Eqs. (4) and (5), respectively; in K] of $Fe_{0.5}M_{0.5}S_2$.

M	c_{11}	c_{12}	T_c	T_c^*
Zn	199.8	59.0	4940	3350
Ru	401.0	41.5	1290	648
Os	430.7	37.7	1340	615

We obtain the Δ-sol band gap at the PBE lattice constant (Table IV) for each M in the hypothetical MS_2 pyrite crystal structure, since the experimental lattice constants for these structures are unknown. Results are listed in Table III in ascending order of the atomic number of M. Hypothetical semiconductor compounds whose band gap is higher than that of FeS_2 include the group II elements—Be, Mg, Ca, Sr, and Ba—as well as the transition metal Cd. For these six potential candidates, we investigate the band gap bowing parameter and whether they are miscible with FeS_2.

Figure 5 shows the band gap bowing effect of alloying pyrite with the six candidates. We observe an increasing trend in the bowing parameter down the group II elements, ranging from 3.1 eV in $(Fe, Be)S_2$ to 6.8 eV in $(Fe, Ba)S_2$. Due to the large bowing effect, band gaps at intermediate compositions are considerably smaller than FeS_2. In Fig. 6, the mixing enthalpy exhibits a similar trend such that the $(Fe, M)S_2$ system becomes increasingly immiscible as M

TABLE III. Δ-sol fundamental gaps for elements that do not form the pyrite structure with S (E_g in eV). The potential candidates are the group II elements (Be, Mg, Ca, Sr, Ba) and Cd.

M	E_g	M	E_g	M	E_g	M	E_g
Be	2.02	Ga	0.20	Rh	0.25	Ta	0.15
Mg	2.50	Ge	0.94	Pd	0.27	W	0.14
Si	0.48	Sr	2.30	Ag	0.28	Re	0.15
Ca	2.46	Y	−0.63	Cd	1.68	Ir	−0.09
Sc	−0.57	Zr	0.87	In	−1.09	Pt	0.24
Ti	0.26	Nb	0.20	Sn	0.93	Au	0.31
V	0.14	Mo	0.15	Ba	2.07	Hg	0.59
Cr	0.12	Tc	0.13	Hf	1.14	Pb	1.33

TABLE IV. Lattice constant (a_0 in Å), bulk modulus (B in GPa), pressure derivative of the bulk modulus (B'), and band gap (E_g in eV) of $Fe_xM_{1-x}S_2$ for candidates M that do not form the pyrite structure with S. The $x = 1$ data set refers to FeS_2.

M	x	a_0	B	B'	E_g
-	1	5.405	156.9	5.47	1.4
Be	0.75	5.443	134.9	4.50	1.0
	0.5	5.480	116.2	4.32	1.0
	0.25	5.514	100.5	4.42	1.1
	0	5.543	88.1	4.10	2.0
Mg	0.75	5.572	123.3	4.39	0.89
	0.5	5.752	97.5	4.60	0.91
	0.25	5.940	77.2	4.57	1.1
	0	6.133	59.9	4.57	2.5
Ca	0.75	5.692	113.8	4.98	0.55
	0.5	6.005	83.2	4.92	0.53
	0.25	6.333	60.5	4.75	0.97
	0	6.678	44.4	4.32	2.5
Sr	0.75	5.761	106.8	4.55	0.24
	0.5	6.158	75.4	5.29	0.31
	0.25	6.580	52.1	4.22	0.75
	0	7.020	37.6	4.53	2.3
Cd	0.75	5.634	123.6	5.23	0.61
	0.5	5.879	96.4	4.48	0.61
	0.25	6.139	74.3	4.81	0.79
	0	6.412	57.1	4.57	1.7
Ba	0.75	5.827	101.7	4.54	0.04
	0.5	6.321	67.4	5.36	0.23
	0.25	6.851	44.1	5.26	0.57
	0	7.403	31.8	4.36	2.1

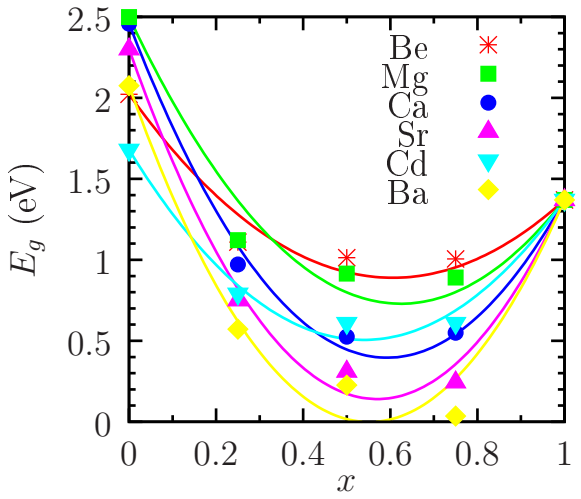

FIG. 5. (Color online) Band gap bowing of $Fe_xM_{1-x}S_2$, where M=Be, Mg, Ca, Sr, Cd, Ba. For group II candidates, the bowing effect becomes more prominent down the group.

goes down group II. The interaction parameter for Be already translates to a critical temperature of 2740 K [Eq. (4)]. Therefore, these materials are unlikely candidates to increase the band gap of pyrite.

IV. DISCUSSION

We have evaluated the potential of a large number of alloying elements to increase the band gap of FeS_2. In addition to the known higher-gap pyrites—ZnS_2, RuS_2, and OsS_2—we also find the group II elements and Cd have larger Δ-sol gaps in the pyrite structure than FeS_2 (Table III). The lattice constants of all these candidate systems closely follow

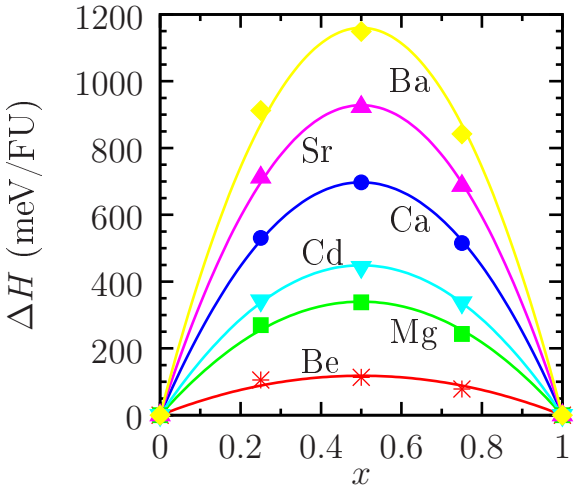

FIG. 6. (Color online) Mixing enthalpy of $Fe_xM_{1-x}S_2$, where M=Be, Mg, Ca, Sr, Cd, Ba. For group II elements, the miscibility decreases down the group.

Vegard's law (Tables I and IV). While small gap bowing ($b_g \approx 0.4$ eV) and band gap enhancement are observed for Ru and Os, large gap bowing is observed in other systems, ranging from 3.1 eV in Be to 6.8 eV in Ba, resulting in a decrease in the band gap of FeS_2 at intermediate alloying concentrations (Figs. 3 and 5). In all candidate systems considered, the mixing enthalpy ΔH is the most limiting quantity, as it inhibits alloying into FeS_2 (Figs. 4 and 6). Even within the most miscible systems, $(Fe, Ru)S_2$ and $(Fe, Os)S_2$, the regular solution critical temperature is around 1300 K, substantially higher than the melting point of FeS_2 (Table II). The problem is further compounded by the fact that the large positive ΔH correlates to large band gap bowing (compare Figs. 3 and 4; Figs. 5 and 6), making all elements that have larger gaps in the (hypothetical) pyrite structure examined in this study ineffective to increase the band gap of pyrite.

The correlation between band gap bowing and miscibility can be traced to differences in ionic radius and electronegativity between the solvent and solute. We shall denote the differences as $\Delta r = r_M - r_{Fe}$ and $\Delta\chi = \chi_M - \chi_{Fe}$, respectively. In Table V we list the calculated band gap bowing parameter and interaction parameter of all examined candidate systems together with their experimental Shannon ionic radius[34] (low spin 2+ charge state in octahedral configuration[3]) and electronegativity.[35] As illustrated in Fig. 7, we observe that the interaction parameter increases with both $\Delta\chi$ and Δr, indicating the $(Fe, M)S_2$ system is less miscible for larger differences in electronegativity or size.

On the other hand, for elements that have been successfully incorporated into pyrite, namely, the transition metals Co, Ni, and Cu (Sec. I),[10,11] the corresponding Shannon ionic radius is 0.65, 0.69, and 0.73 Å,[34] and the electronegativity is 1.88, 1.91, and 1.90.[35] The differences compared to Fe are $\Delta r = 0.04$, 0.08, and 0.12 Å, and $\Delta\chi = 0.05$, 0.08, and 0.07, respectively, for Co, Ni, and Cu. Therefore, Co is expected to be the most soluble element within pyrite. Indeed, it has been experimentally demonstrated that Co forms a solid solution with pyrite at all compositions.[10] $Fe_xNi_{1-x}S_2$ has also been synthesized for $0.4 \leq x \leq 0.6$, showing substantial solubility.[11] As for Cu, although its electronegativity is similar to that of Fe, the ionic radius difference is 0.12 Å, comparable to Mg and Zn (Table V). A limited solubility is exhibited in $Fe_xCu_{1-x}S_2$, where compositions of only $0.16 \leq x \leq 0.27$ are achieved.[11] Despite their different degrees of solubility, the Co, Ni, and Cu disulfides have lower band gaps,[2] and are not suitable for the band gap enhancement of pyrite, as pointed out in Sec. I. The next element in the transition metal series, Zn, has a comparable size difference as Cu ($\Delta r = 0.13$ Å) and a larger estimated band gap (2.5 eV; Ref. 8) that is verified computationally (2.1 eV; Table I). However, in this case, its electronegativity difference of 0.18 makes ZnS_2 highly immiscible with FeS_2 and causes a large band gap bowing as shown in Fig. 3. Based on our results, we question whether Zn can really be effective in increasing the band gap and OCV of pyrite, as proposed by Altermatt *et al.*[7] [Note that natural impurities typically occur below $O(10^{19})$ cm^{-3} in pyrite; see Refs. 2 and 4.] The strong positive correlations between miscibility and differences in ionic radius and electronegativity observed in this study may serve as general guiding rules in materials design for band gap engineering in other systems.

We remark on the improvement of calculated band gaps using the Δ-sol method. The GGA band structures of ZnS_2, RuS_2, and OsS_2 are shown in Fig. 8. (See Ref. 3 for the band structure of FeS_2.) Going down the Fe column in the periodic table (Fe, Ru, Os), the experimental band gap increases monotonically from 0.95, 1.3, to 2.0 eV. The Kohn-Sham gap [$\epsilon_{CBM} - \epsilon_{VBM}$, which is the difference in eigenvalues at the conduction band minimum (CBM) and valence band maximum (VBM)] down the group is, respectively, 0.4, 0.4, and -0.07 eV, which corresponds to an

TABLE V. Shannon ionic radius[34] (r) and electronegativity[35] (χ) of M, and band gap bowing parameter (b_g) and interaction parameter (Ω) of (Fe, M)S_2. Data for Fe are shown in the first row. The ionic radii of Ru^{2+} and Os^{2+} are not available.

M	r (Å)	χ	b_g (eV)	Ω (meV/FU)
-	0.61	1.83	-	-
Be	0.45	1.57	3.1	473
Mg	0.72	1.31	4.5	1360
Ca	1.00	1.00	5.9	2790
Zn	0.74	1.65	3.3	851
Sr	1.18	0.95	6.6	3710
Ru	-	2.2	0.44	222
Cd	0.95	1.69	4.1	1800
Ba	1.35	0.89	6.8	4640
Os	-	2.2	0.41	231

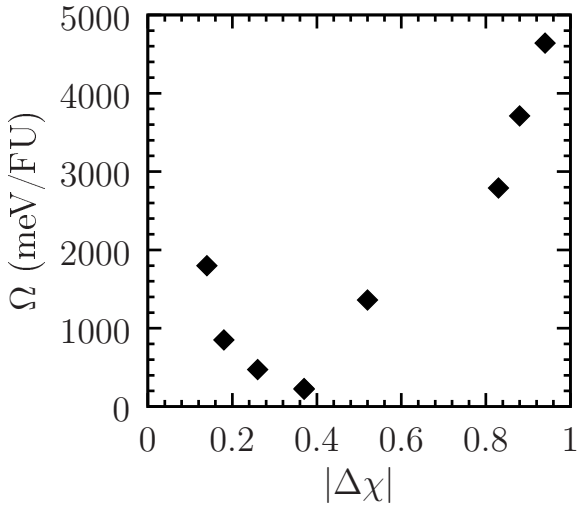

(a)

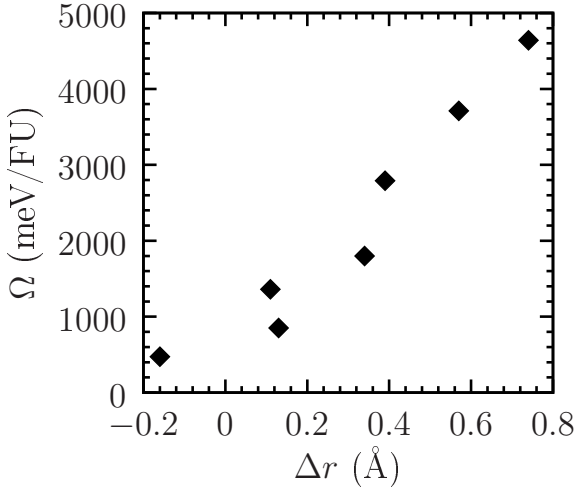

(b)

FIG. 7. Interaction parameter (Ω) as a function of (a) difference in electronegativity[35] ($\Delta\chi$); and (b) difference in Shannon ionic radius[34] (Δr). Ru and Os are not plotted in (b) because their Shannon ionic radii in the 2+ state are not available.

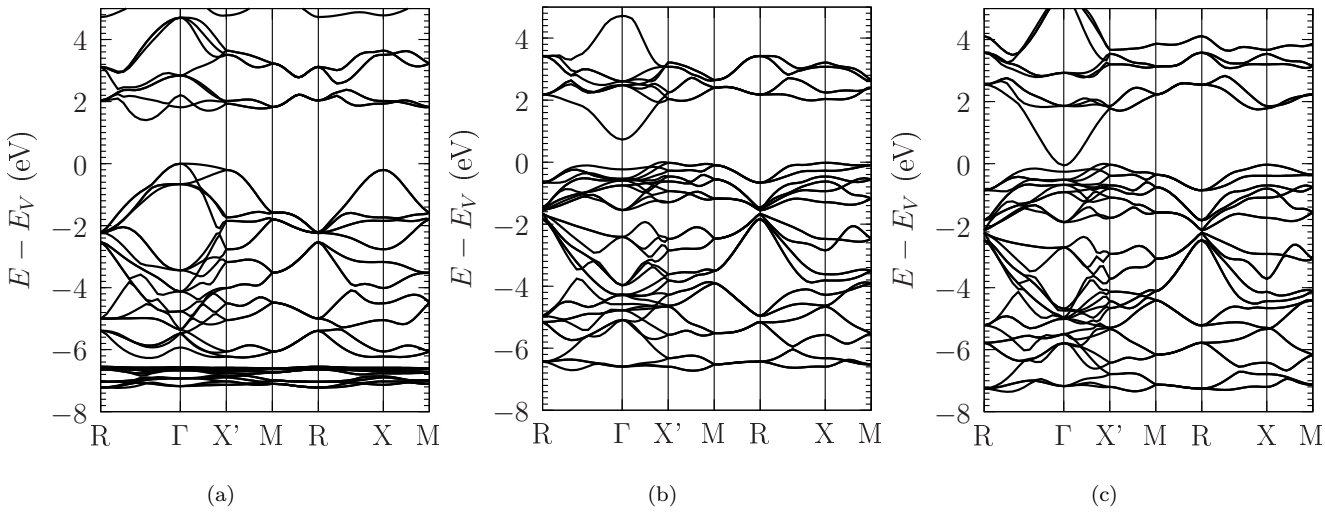

FIG. 8. Band structure of (a) ZnS_2; (b) RuS_2; and (c) OsS_2.

increasingly severe underestimation of 0.55 (−58%), 0.9 (−69%), and 2 eV (−100%), as listed in Table I. This trend is in direct contradiction to the common belief that *relative* Kohn-Sham gaps within a chemically similar family of materials should be in reasonable agreement with experiment. On the other hand, the Δ-sol method yields band gaps of 1.4 (+47%), 1.8 (+38%), and 1.8 eV (−10%), respectively, showing substantial improvement in both the accuracy as well as the qualitative trend.

Due to the significant discrepancy between the Kohn-Sham gap and the experimental gap, an *ad hoc* correction is usually made such that the band gaps of the end members are fixed at their experimental gaps, and the gaps at intermediate compositions are adjusted by linear interpolation of the gap errors at $x = 0$ and $x = 1$. This GGA band gap correction scheme can be found in, e.g., Ref. 36. One may question whether the implementation of such an interpolation scheme would affect our results, since the pyrite band gap is calculated to be 1.4 eV within the Δ-sol method, which is 0.45 eV higher than the experimental value,[2] and a downward shift at $x = 1$ in Fig. 5 would seem to make the candidate systems more effective. However, we do not show such corrections in this study for three reasons. (i) The band gap bowing parameter is obtained by fitting the calculated band gaps to a quadratic function and it is independent of a linear correction term. (ii) The band gap at $x = 0.5$ is significantly smaller than that of both end members for most of the materials examined here, yielding a substantial bowing parameter. Since the bowing parameter [$O(1)$ eV] is much larger than the mean error in the Δ-sol gap [$O(0.1)$ eV],[24] the band gap would decrease with solute concentration near the FeS_2 end member regardless of whether the correction is applied. Thus, the conclusion of whether a candidate is feasible would remain the same even if the correction scheme were to be adopted. (iii) The experimental band gaps for the non-isostructural candidates in the pyrite structure are unknown. It would be inconsistent to use experimental gaps at one end (Fe limit) and computed gaps at the other (M limit).

Only ordered structures have been used in our calculations. Due to the fact that the cation sites form a face-centered cubic sublattice,[3] there is only one unique configuration at $x = 0.25$, 0.5, and 0.75 for the unit cell. One may wonder if random cation arrangements would give substantially different results. Special quasirandom structures (SQS) are commonly used to simulate the structure of a random alloy using a small supercell (typically $2 \times 2 \times 2$) whose correlation function closely approximates that of an ideal random alloy for a given concentration.[37] We have tested the case of $(Fe, Zn)S_2$, using the initial structure generated by von Pezold *et al.*[38] within the Alloy Theoretic Automated Toolkit (ATAT) code.[39] The ionically-relaxed mixing enthalpy obtained from the SQS approach is even higher than that obtained from the unit cell approach. Given that the mixing enthalpy ΔH obtained from the latter is already highly limiting for all systems, we have not carried out further investigations on the configurational effects using the SQS approach. For the same reason, the $\Delta H_{p' \to \text{pyrite}}$ term in Eq. (8) has not been evaluated. We do recommend that, however, if a successful candidate were identified from the screening procedure, then more detailed analyses of the phase stability and ordering effects should be performed.

While our results offer a pessimistic perspective on the likelihood of increasing the band gap of FeS_2, it is important to note that there are some possibilities that we have not considered:

(i) *Anion mixing.* Isovalent alternatives for the anion are very limited. $FeSe_2$ and $FeTe_2$ crystallize in the marcasite phase and are non-isostructural to pyrite.[40] The experimental band gap of the diselenide varies from 0.5 to 1 eV,[40,41]

and that of the ditelluride is even smaller,[40] which is undesirable.

(ii) *Mixing in both sites.* Isostructural diselenides and ditellurides include the compounds of such elements as Mn, Ru, Os, and Co.[2] The $(Fe, M)(S, A)_2$ class of materials, where M is one of the above transition metals and A=Se or Te, has not been studied. Unfortunately, the toxicity and scarcity of these chalcogens would make them unfavorable for large-scale photovoltaic applications.

(iii) *Mixtures of alloying cations of the form* $(Fe, M, N)S_2$. Here the combined aliovalent alloying elements M and N should average to a 2+ charge. However, it is likely that a large addition of such elements will lead to the formation of intermediate compounds due to the effective electrostatic interaction between cations of different charge.[42]

Finally, it has also been amply demonstrated that high supersaturation of alloying elements can be achieved in materials with far-from-equilibrium techniques such as pulsed-laser melting.[43] In these situations the spinodal instability will play a key role in the reliability and durability of the synthesized product.

V. CONCLUSIONS

The feasibility of alloying pyrite FeS_2 to enhance its band gap is investigated from first-principles. Among the isostructural candidates (Zn, Ru, Os), band gap enhancement is observed for Ru and Os, but they are expected to exhibit poor miscibility. Using a materials screening procedure, we identify six non-isostructural candidates, namely, the group II elements (Be, Mg, Ca, Sr, Ba) and Cd, that have larger band gaps in the pyrite structure compared to FeS_2. Large band gap bowing effects are found in these systems, making them ineffective to enhance the band gap of pyrite. We also observe positive correlations between immiscibility and differences in the ionic radius and electronegativity.

ACKNOWLEDGMENTS

This work was funded by the Chesonis Family Foundation under the Solar Revolution Project and the U.S. Department of Energy under Contract No. DE-FG02-05ER46253.

* gceder@mit.edu

[1] W. Shockley and H. Queisser, J. Appl. Phys., **32**, 510 (1961).
[2] A. Ennaoui, S. Fiechter, C. Pettenkofer, N. Alonso-Vante, K. Büker, M. Bronold, C. Höpfner, and H. Tributsch, Sol. Energy Mater. Sol. Cells, **29**, 289 (1993).
[3] R. Sun, M. K. Y. Chan, and G. Ceder, Phys. Rev. B, **83**, 235311 (2011).
[4] R. Sun, M. K. Y. Chan, S. Y. Kang, and G. Ceder, Phys. Rev. B, **84**, 035212 (2011).
[5] S.-H. Wei and A. Zunger, J. Appl. Phys., **78**, 3846 (1995).
[6] I. Vurgaftman, J. R. Meyer, and L. R. Ram-Mohan, J. Appl. Phys., **89**, 5815 (2001).
[7] P. P. Altermatt, T. Kiesewetter, K. Ellmer, and H. Tributsch, Sol. Energy Mater. Sol. Cells, **71**, 181 (2002).
[8] D. Bullett, J. Phys. C, **15**, 6163 (1982).
[9] A. Fujimori, K. Mamiya, T. Mizokawa, T. Miyadai, T. Sekiguchi, H. Takahashi, N. Môri, and S. Suga, Phys. Rev. B, **54**, 16329 (1996).
[10] R. J. Bouchard, Mater. Res. Bull., **3**, 563 (1968).
[11] T. A. Bither, P. C. Donohue, W. H. Cloud, P. E. Bierstedt, and H. S. Young, J. Solid State Chem., **1**, 526 (1970).
[12] P. Hohenberg and W. Kohn, Phys. Rev., **136**, B864 (1964).
[13] W. Kohn and L. J. Sham, Phys. Rev., **140**, A1133 (1965).
[14] J. P. Perdew, K. Burke, and M. Ernzerhof, Phys. Rev. Lett., **77**, 3865 (1996).
[15] J. P. Perdew, K. Burke, and M. Ernzerhof, Phys. Rev. Lett., **78**, 1396 (1997).
[16] G. Kresse and J. Hafner, Phys. Rev. B, **47**, 558 (1993).
[17] G. Kresse and J. Hafner, Phys. Rev. B, **49**, 14251 (1994).
[18] G. Kresse and J. Furthmüller, Phys. Rev. B, **54**, 11169 (1996).
[19] G. Kresse and J. Furthmüller, Comput. Mater. Sci., **6**, 15 (1996).
[20] P. E. Blöchl, Phys. Rev. B, **50**, 17953 (1994).
[21] G. Kresse and D. Joubert, Phys. Rev. B, **59**, 1758 (1999).
[22] H. J. Monkhorst and J. D. Pack, Phys. Rev. B, **13**, 5188 (1976).
[23] F. Murnaghan, P. Natl. Acad. Sci. USA, **30**, 244 (1944).
[24] M. K. Y. Chan and G. Ceder, Phys. Rev. Lett., **105**, 196403 (2010).
[25] J. Heyd, G. E. Scuseria, and M. Ernzerhof, J. Chem. Phys., **118**, 8207 (2003).
[26] J. Heyd, G. E. Scuseria, and M. Ernzerhof, J. Chem. Phys., **124**, 219906 (2006).

[27] I. P. Ipatova, V. G. Malyshkin, and V. A. Shchukin, J. Appl. Phys., **74**, 7198 (1993).
[28] M. J. Mehl, Phys. Rev. B, **47**, 2493 (1993).
[29] C. Wadia, A. P. Alivisatos, and D. M. Kammen, Environ. Sci. Technol., **43**, 2072 (2009).
[30] K. Persson, G. Ceder, and D. Morgan, Phys. Rev. B, **73**, 115201 (2006).
[31] R. Murphy and D. R. Strongin, Surf. Sci. Rep., **64**, 1 (2009).
[32] H. Lutz, B. Muller, T. Schmidt, and T. Stingl, Acta Crystallogr. C, **46**, 2003 (1990).
[33] T. Stingl, B. Mueller, and H. Lutz, Z. Kristallogr., **202**, 161 (1992).
[34] R. D. Shannon, Acta Crystallogr. A, **32**, 751 (1976).
[35] A. L. Allred, J. Inorg. Nucl. Chem., **17**, 215 (1961).
[36] S. Chen, X. G. Gong, and S.-H. Wei, Phys. Rev. B, **75**, 205209 (2007).
[37] A. Zunger, S.-H. Wei, L. G. Ferreira, and J. E. Bernard, Phys. Rev. Lett., **65**, 353 (1990).
[38] J. von Pezold, A. Dick, M. Friák, and J. Neugebauer, Phys. Rev. B, **81**, 094203 (2010).
[39] A. van de Walle, M. Asta, and G. Ceder, Calphad, **26**, 539 (2002).
[40] T. Harada, J. Phys. Soc. Jpn., **67**, 1352 (1998).
[41] H. Kwon, S. Thanikaikarasan, T. Mahalingam, K. Park, C. Sanjeeviraja, and Y. Kim, J. Mater. Sci.-Mater. El., **19**, 1086 (2008).
[42] G. Ceder, G. D. Garbulsky, and P. D. Tepesch, Phys. Rev. B, **51**, 11257 (1995).
[43] M.-J. Sher, M. T. Winkler, and E. Mazur, MRS Bull., **36**, 439 (2011).